


# Alterations in Cerebral Cortical Glucose and Glutamine Metabolism Precedes Amyloid Plaques in the APP<sup>swe</sup>/PSEN1<sup>dE9</sup> Mouse Model of Alzheimer's Disease

Jens V. Andersen<sup>1</sup> · Sofie K. Christensen<sup>1</sup> · Blanca I. Aldana<sup>1</sup> · Jakob D. Nissen<sup>1</sup> · Heikki Tanila<sup>2</sup> · Helle S. Waagepetersen<sup>1</sup> 

Received: 5 September 2016 / Revised: 21 September 2016 / Accepted: 22 September 2016 / Published online: 29 September 2016  
© Springer Science+Business Media New York 2016

**Abstract** Alterations in brain energy metabolism have been suggested to be of fundamental importance for the development of Alzheimer's disease (AD). However, specific changes in brain energetics in the early stages of AD are poorly known. The aim of this study was to investigate cerebral energy metabolism in the APP<sup>swe</sup>/PSEN1<sup>dE9</sup> mouse prior to amyloid plaque formation. Acutely isolated cerebral cortical and hippocampal slices of 3-month-old APP<sup>swe</sup>/PSEN1<sup>dE9</sup> and wild-type control mice were incubated in media containing [U-<sup>13</sup>C]glucose, [1,2-<sup>13</sup>C]acetate or [U-<sup>13</sup>C]glutamine, and tissue extracts were analyzed by mass spectrometry. The ATP synthesis rate of isolated whole-brain mitochondria was assessed by an on-line luciferin-luciferase assay. Significantly increased <sup>13</sup>C labeling of intracellular lactate and alanine and decreased tricarboxylic acid (TCA) cycle activity were observed from cerebral cortical slices of APP<sup>swe</sup>/PSEN1<sup>dE9</sup> mice incubated in media containing [U-<sup>13</sup>C]glucose. No changes in glial [1,2-<sup>13</sup>C]acetate metabolism were observed. Cerebral cortical slices from APP<sup>swe</sup>/PSEN1<sup>dE9</sup> mice exhibited a reduced capacity for uptake and oxidative metabolism of glutamine. Furthermore, the ATP synthesis rate tended to be decreased in isolated whole-brain mitochondria of APP<sup>swe</sup>/PSEN1<sup>dE9</sup> mice. Thus, several cerebral metabolic changes

are evident in the APP<sup>swe</sup>/PSEN1<sup>dE9</sup> mouse prior to amyloid plaque deposition, including altered glucose metabolism, hampered glutamine processing and mitochondrial dysfunctions.

**Keywords** Brain energy metabolism · Alzheimer's disease · APP<sup>swe</sup>/PSEN1<sup>dE9</sup> · Mitochondria · Glutamine

## Abbreviations

ACSF	Artificial cerebrospinal fluid
AD	Alzheimer's disease
GS	Glutamine synthetase
M	Molecular ion
MCL	Molecular carbon labeling
PAG	Phosphate-activated glutaminase
PDH	Pyruvate dehydrogenase
TG	Transgene

## Introduction

Alzheimer's disease (AD) is a complex neurodegenerative disorder causing progressive deterioration of cognitive functions leading to dementia. A molecular hallmark of AD is cerebral accumulation of amyloid  $\beta$ -peptide and further deposition in amyloid plaques. The formation of amyloid plaques is regarded as a main factor of AD pathology and has been associated with several cerebral complications including inflammation, oxidative stress and mitochondrial dysfunction [1, 2]. Alterations in cerebral glucose metabolism have been observed in individuals prone to familial AD before manifestation of amyloid plaques, suggesting that changes in brain energy metabolism might be causative of AD development [2–4]. Yet,

Special Issue: In honour of Ursula Sonnewald.

✉ Helle S. Waagepetersen  
Helle.Waagepetersen@sund.ku.dk

<sup>1</sup> Department of Drug Design and Pharmacology, Faculty of Health and Medical Sciences, University of Copenhagen, Copenhagen, Denmark

<sup>2</sup> A. I. Virtanen Institute for Molecular Sciences, University of Eastern Finland, Kuopio, Finland

specific changes in AD brain energetics prior to amyloid plaque manifestation are poorly known. Accordingly, we decided to investigate if alterations in brain energy metabolism were present before amyloid plaque formation in the widely used AD mouse model, the APPsw/PSEN1dE9 mouse.

This mouse model of AD expresses two familial AD mutations causing an aggressive formation of insoluble amyloid plaques in the brain [5]. The disease progression in these mice is well characterized. The first amyloid plaques develop around 4 months of age [6], while memory impairment manifests around 12 months of age [7–9]. In addition, these mice show an epileptic phenotype and preterm mortality that peaks around 3 months of age [10].

Glucose is the main energy substrate of both neurons and glial cells. Hampered cerebral glucose utilization is associated with cognitive dysfunctions [4]. Alterations in glycolysis and oxidative metabolism have been reported in the AD brain [2, 3]. Neurons and glial cells function in tight cooperation in the brain, a prime example being the glutamate-glutamine cycle [11]. Released neurotransmitter glutamate is mainly taken up by astrocytes and converted into glutamine, which is subsequently transported back to the neurons. Glutamine is deamidated into glutamate in the neuron, and the cycle is thereby complete. The glutamate-glutamine cycle is linked to cellular energy metabolism as glutamate can be converted into  $\alpha$ -ketoglutarate and serve as substrate for the tricarboxylic acid (TCA) cycle. To investigate whether glucose and glutamine metabolism could be impaired prior to amyloid plaque manifestation, we incubated acutely isolated brain slices from 3-month-old APPsw/PSEN1dE9 mice with different  $^{13}\text{C}$  labeled energy substrates.

The main production of ATP takes place by oxidative phosphorylation in mitochondria. It has been proposed that malfunction of cerebral mitochondria plays a major role in the metabolic changes observed in the AD brain [2, 12, 13]. To elucidate if mitochondria are affected prior to the development of amyloid plaques in the brain of the APPsw/PSEN1dE9 mouse, the ATP production rate of isolated brain mitochondria was assessed.

## Materials and Methods

### Isotopes and Chemicals

[U- $^{13}\text{C}$ ]glucose (99%) and [U- $^{13}\text{C}$ ]glutamine (99%) were purchased from Cambridge Isotope Laboratories (Tewksbury, MA, USA) and [1,2- $^{13}\text{C}$ ]acetate (99%) was purchased from ISOTECH<sup>®</sup> (Miamisburg, OH, USA). All other chemicals used were of the purest grade available from commercial sources.

### Animals

Transgenic mice carrying mouse/human amyloid precursor protein with the Swedish mutation and deletion of exon 9 of human presenilin-1 (APPsw/PSEN1dE9 mice) were originally generated by D. Borchelt and J. Jankowsky at Johns Hopkins University, Baltimore, MD, USA [5]. Mice for this study were obtained from a colony at the University of Eastern Finland. The mice were practically of pure C57Bl/6J background after more than 15 generations of backcrossing to this strain. Young adult (3 months) male APPsw/PSEN1dE9 mice and wild-type control littermates were used in these experiments. The animals were kept in humidity and temperature controlled facility, with 12/12 h light/dark cycle with free access to water and chow. All experiments were approved by the Danish National Ethics Committee and were performed according to the European Convention ETS 123 of 1986.

### Brain Slice Preparation and Incubations

Animals were euthanized by cervical dislocation and decapitated. The brain was removed and submerged in ice-cold artificial cerebrospinal fluid (ACSF), containing in mM: NaCl 128, NaHCO<sub>3</sub> 25, D-glucose 10, KCl 3, CaCl<sub>2</sub> 2, MgSO<sub>4</sub> 1.2, KH<sub>2</sub>PO<sub>4</sub> 0.4, pH 7.4. The cortices and hippocampi were dissected and sliced (350  $\mu\text{m}$ ) using a McIlwain tissue chopper (The Vibratome Company, O'Fallon, MO, USA). Two cortical or six hippocampal slices were placed in each chamber and allowed to recover from slicing, by incubation in ACSF for 60 min. Subsequently, the slices were incubated for 60 min in ACSF (without 10 mM D-glucose) containing either 5 mM [U- $^{13}\text{C}$ ]glucose, 5 mM [1,2- $^{13}\text{C}$ ]acetate and 5 mM D-glucose or 1 mM [U- $^{13}\text{C}$ ]glutamine and 5 mM D-glucose. The incubations were terminated by transferring slices to ice-cold 70% ethanol. The slices were sonicated, centrifuged (20,000g  $\times$  20 min) and the supernatant removed. Pellets were saved for protein determination (Pierce method) while the supernatant was lyophilized and reconstituted in water for determination of  $^{13}\text{C}$  labeling of metabolites and quantification of amino acids, by GC-MS and HPLC analysis, respectively.

### Gas Chromatography Mass Spectrometry (GC-MS)

#### Analysis

Aqueous extracts of brain slices were acidified, to pH 1–2, with HCl and evaporated to dryness under nitrogen flow. Organic extraction was carried out twice, using 96% ethanol and benzene, with evaporation to dryness under nitrogen flow between the two extractions. TCA cycle intermediates and amino acids in the samples were derivatized using N-tert-butyltrimethylsilyl-N-methyl-trifluoroacetamide in

the presence of dimethylformamide. The samples were analyzed by gas chromatography (Agilent Technologies 7820A, J&W GC column HP-5MS) coupled to a mass spectrometer (Agilent Technologies 5977E). Isotopic enrichment was corrected for the natural abundance of  $^{13}\text{C}$  by standards containing unlabeled metabolites of interest. Data are presented as %  $^{13}\text{C}$  enrichment of  $M+X$ , where  $M$  is the molecular ion of the given molecule and  $X$  is the number of  $^{13}\text{C}$  atoms in the molecule or as molecular carbon labeling (MCL) an average of total  $^{13}\text{C}$  enrichment in the given molecule [14].

### High Performance Liquid Chromatography (HPLC) Analysis

Quantitative amounts of amino acids in brain slice extracts were determined by reverse phase high performance liquid chromatography (Agilent Technologies 1260 Infinity, Agilent ZORBAX Eclipse plus C18 column). Pre-column o-phthalaldehyde derivatization and fluorescent detection (excitation  $\lambda=338$  nm, emission  $\lambda=390$  nm) were performed. Gradient elution with aqueous mobile phase A (10 mM  $\text{NaH}_2\text{PO}_4$ , 10 mM  $\text{Na}_2\text{B}_4\text{O}_7$ , 0.5 mM  $\text{NaN}_3$ , pH 8.2) and mobile phase B (acetonitrile 45%: methanol 45%:  $\text{H}_2\text{O}$  10%, V:V:V), was used. Mobile phase B increased linearly from 2 to 57% from 0 to 30 min, then from 57 to 100% in 0.1 min, to return again to 2% in minute 33.6 with a total run time of 35 min. The amounts of amino acids were determined from standards containing amino acids of interest.

### Lactate Determination

Lactate released from brain slices to the medium was assessed by a lactate-kit from Boehringer Mannheim/R-Biopharm AG (Darmstadt, Germany), according to the manufacturer's instructions.

### Mitochondrial Isolation and ATP Synthesis Rate Assay

Whole-brain mitochondria of wild-type control and APPswe/PSEN1dE9 mice were isolated in tandem for each experiment using a Percoll gradient. All procedures were performed on ice or at 4°C. Animals were euthanized by cervical dislocation and decapitated. The brain was quickly removed and placed in cold mitochondrial isolation buffer containing in mM: mannitol 210, sucrose 70, HEPES 5, EGTA 1 and 0.5% BSA (fatty acid free), pH 7.2, and homogenized using a Teflon douncer, 750 revolutions/min, 7–8 strokes. The homogenate was centrifuged, 500g  $\times$  5 min, and the pellet was discarded. The supernatant was centrifuged, 14,000g  $\times$  10 min, and the pellet was re-suspended in 12% Percoll solution. This suspension was gently layered on top of 21% Percoll solution and centrifuged, 18,000g  $\times$  15 min. The supernatant was discarded and the mitochondrial

fraction was rinsed with two subsequent centrifugations (18,000g  $\times$  5 and 14,000g  $\times$  5 min) by suspending the mitochondria in isolation buffer and discarding the supernatant after each centrifugation. The mitochondrial pellet was re-suspended in isolation buffer and the amount of protein was determined (Bradford method). The ATP synthesis assay measures luminescence from the reaction of ATP and luciferin, catalyzed by luciferase, using a NOVOstar plate reader (BMG Labtech, Ortenberg, Germany). The isolated mitochondria were diluted in respiration buffer, containing in mM: sucrose 250,  $\text{K}_2\text{HPO}_4$  15,  $\text{MgSO}_4$  2, EDTA 0.5 and 0.5% BSA (fatty acid free), pH 7.2 and 2.5  $\mu\text{g}$  of protein were added to each well. The wells contained pyruvate and P1,P5-diadenosine pentaphosphate in final concentrations of 5 mM and 10  $\mu\text{M}$ , respectively. During the measurement period, three injections were performed: firstly a luciferin-luciferase cocktail was injected, to establish the background luminescence. Following, 2 mM ADP in combination with 2.5 mM malate (final concentrations), were injected and finally 250  $\mu\text{M}$  ATP was injected, as an internal standard for determination of the produced amount of ATP. The apparatus and suspensions were preheated to 28°C for optimal luciferin-luciferase response. The results are presented as the rate of ATP synthesis in nmol/(min\*mg).

### Statistical Analysis

Data are presented as mean  $\pm$  standard error of the mean (SEM). Significant outliers were identified by Grubbs' test ( $\alpha=0.05$ ). Student's unpaired  $t$  test was employed to test if differences were statistically significant. The significance level was set at  $p < 0.05$  and is indicated with a single asterisk.

## Results

### Amino Acid Amounts in Brain Slices of APPswe/PSEN1dE9 Mice

We observed no significant differences between APPswe/PSEN1dE9 and wild-type control mice in amino acid amounts (glutamine, glutamate, aspartate, GABA and alanine) in extracts of cerebral cortical or hippocampal slices incubated in media containing [ $^{13}\text{C}$ ]glucose (Fig. 1a, b) or [ $^{13}\text{C}$ ]acetate (data not shown). However, changes in amino acid contents were found between cerebral cortex slices of wild-type control and APPswe/PSEN1dE9 mice incubated in media containing [ $^{13}\text{C}$ ]glutamine (Fig. 1c). Significantly lower levels of glutamine (40%) and aspartate (31%), and a tendency towards lower glutamate ( $p=0.170$ ) were observed for cerebral cortical slices of APPswe/PSEN1dE9 mice when compared to wild-type controls.

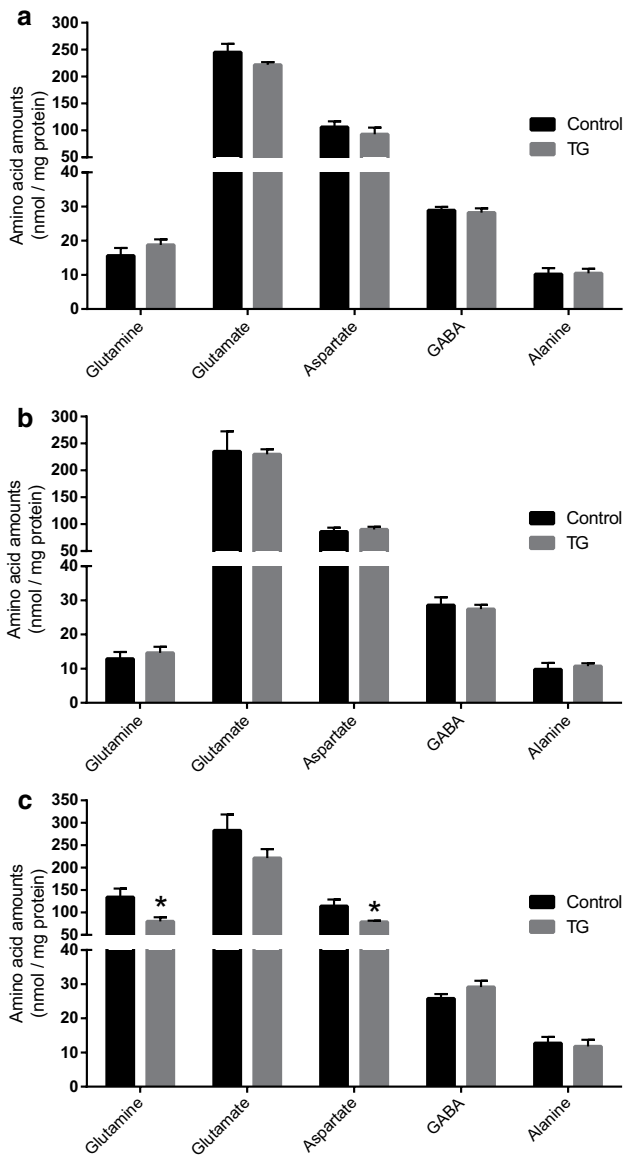


**Fig. 1** Amino acid amounts of brain slice extracts. Amino acid contents of cerebral cortical (a) and hippocampal (b) slices of wild-type control and APPsw/PSEN1dE9 (TG) mice incubated in media containing [U-<sup>13</sup>C]glucose. Amino acid contents of cerebral cortical (c) slices of wild-type control and APPsw/PSEN1dE9 (TG) mice incubated in media containing [U-<sup>13</sup>C]glutamine. Results are presented as mean ± SEM, n=4–5. Student's *t* test, *p* < 0.05

The decreased amount of intracellular glutamine, from the incubations with exogenously added [U-<sup>13</sup>C]glutamine, indicates an impairment of glutamine uptake capacity, in cerebral cortical slices of APPsw/PSEN1dE9 mice.

### Alterations in Glucose Metabolism in Cerebral Cortical Slices of APPsw/PSEN1dE9 Mice

<sup>13</sup>C Labeling of metabolites generated from glycolysis and first turn of the TCA cycle obtained from incubations of

cerebral cortex and hippocampus slices of wild-type control and APPsw/PSEN1dE9 mice in medium containing [U-<sup>13</sup>C]glucose are presented in Fig. 2. [U-<sup>13</sup>C]glucose is metabolized through glycolysis into [U-<sup>13</sup>C]pyruvate, which can subsequently be converted into lactate M+3, alanine M+3 or be transported into mitochondria. In the mitochondria [U-<sup>13</sup>C]pyruvate may be oxidatively decarboxylated into [1,2-<sup>13</sup>C]acetylCoA catalyzed by pyruvate dehydrogenase (PDH) and upon entry in the TCA cycle give rise to M+2 labeled metabolites.

Significant increases in lactate M+3 (205%) and alanine M+3 (45%) labeling were observed for the cerebral cortex slices of APPsw/PSEN1dE9 mice when compared to wild-type controls (Fig. 2a). Significant increases in <sup>13</sup>C labeling were also observed for several first turn TCA cycle intermediates including: citrate M+2 (14%), α-ketoglutarate M+2 (71%), succinate M+2 (100%), fumarate M+2 (55%) and malate M+2 (40%) in the cerebral cortex slices of APPsw/PSEN1dE9 mice. Additionally, a significant increased labeling of glutamine M+2 (10%) was observed. None of these changes were observed in hippocampal slices of APPsw/PSEN1dE9 mice (Fig. 2b). We were not able to pick up a significant difference in the amounts of lactate released from slices to the media during the incubations. However, a tendency towards increased lactate release from cerebral cortical slices of APPsw/PSEN1dE9 mice when compared to wild-type controls, was observed ( $643.0 \pm 131.7$  vs.  $570.9 \pm 58.9$  nmol lactate/mg protein, *p* = 0.625).

The rate of TCA cycling can be calculated by dividing the percentage of <sup>13</sup>C labeling of later turns isotopologues (i.e. M+3, M+4, M+5 etc.) with the percentage of <sup>13</sup>C labeling of the first turn isotopologue M+2 of TCA cycle intermediates and amino acids. No changes in cycling ratios of hippocampal slices were found (data not shown). Cycling ratios from cerebral cortex slices incubated in media containing [U-<sup>13</sup>C]glucose from wild-type control and APPsw/PSEN1dE9 mice are presented in Fig. 3. The TCA cycling ratios of the cerebral cortical slices were significantly decreased for malate, aspartate, glutamate and glutamine and the same tendency is present for several other TCA cycle intermediates, demonstrating a reduced rate of TCA cycling in cerebral cortical slices of APPsw/PSEN1dE9 mice. Taken together the results obtained from the incubations with [U-<sup>13</sup>C]glucose point towards an altered metabolism of glucose resulting in elevated levels of labeled pyruvate and subsequently labeling of lactate M+3 and alanine M+3 in cerebral cortex slices of APPsw/PSEN1dE9 mice. Additionally, the TCA cycle activity is decreased in the cerebral cortex. These changes are absent in the hippocampus suggesting that glucose metabolism in this region is less affected prior to manifestation of amyloid plaques in the APPsw/PSEN1dE9 mouse.

**Fig. 2** <sup>13</sup>C Labeling from [U-<sup>13</sup>C]glucose metabolism. Labeling of metabolites and amino acids generated from glycolysis and first turn of the TCA cycle from incubations of cerebral cortical (a) and hippocampal (b) slices from wild-type control and APPswe/PSEN1dE9 (TG) mice in media containing [U-<sup>13</sup>C]glucose. Results are presented as mean ± SEM, n=4–5. Student's *t* test, *p* < 0.05

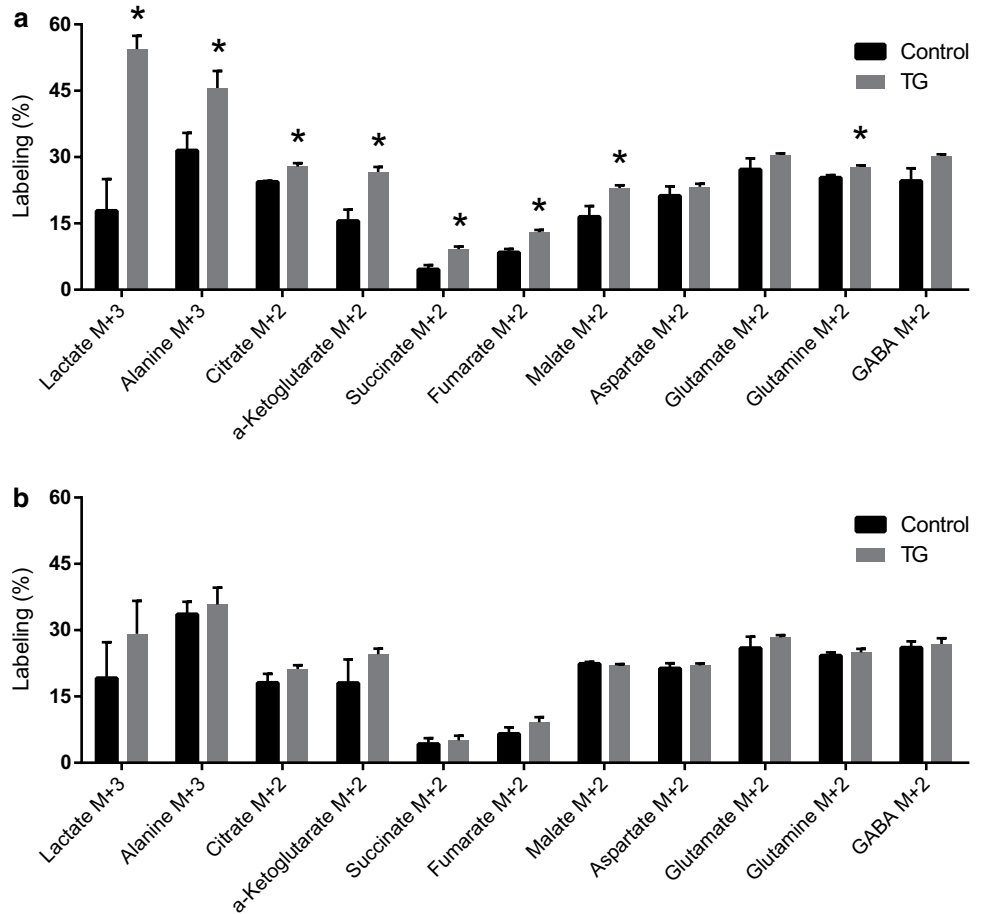
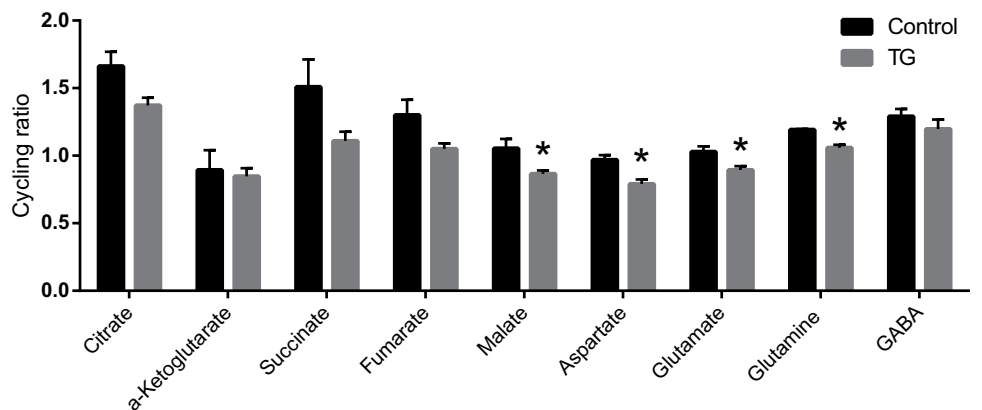


**Fig. 3** Cycling ratios from [U-<sup>13</sup>C]glucose metabolism. TCA cycling ratios obtained from incubations of cerebral cortical slices from wild-type control and APPswe/PSEN1dE9 (TG) mice in media containing [U-<sup>13</sup>C]glucose. Results are presented as mean ± SEM, n=4–5. Student's *t* test, *p* < 0.05



**Unchanged acetate metabolism in brain slices of APPswe/PSEN1dE9 mice**

Molecular carbon labeling (MCL) of TCA cycle intermediates and amino acids obtained from incubations of cerebral cortex and hippocampus slices from wild-type control and APPswe/PSEN1dE9 mice in medium containing [1,2-<sup>13</sup>C]acetate are presented in Fig. 4. [1,2-<sup>13</sup>C]Acetate enters the TCA cycle as [1,2-<sup>13</sup>C]acetylCoA and is predominantly metabolized in

glial cells [15, 16]. No significant differences in MCL were observed for cerebral cortical or hippocampal slices of wild-type control and APPswe/PSEN1dE9 mice incubated in media containing [1,2-<sup>13</sup>C]acetate. In addition, no changes were observed in TCA cycling ratios from metabolism of [1,2-<sup>13</sup>C]acetate (data not shown). These results indicate little or no change in total glial acetate metabolism and TCA cycling in the early stage of amyloid plaque development in APPswe/PSEN1dE9 mice.

**Fig. 4**  $^{13}\text{C}$  Labeling from  $[1,2-^{13}\text{C}]$ acetate metabolism. Molecular carbon labeling of TCA cycle intermediates and amino acids from incubations of cerebral cortical (a) and hippocampal (b) slices from wild-type control and APP<sup>sw</sup>/PSEN1<sup>dE9</sup> (TG) mice in media containing  $[1,2-^{13}\text{C}]$ acetate. Results are presented as mean  $\pm$  SEM,  $n=4-5$ . Student's  $t$  test,  $p < 0.05$

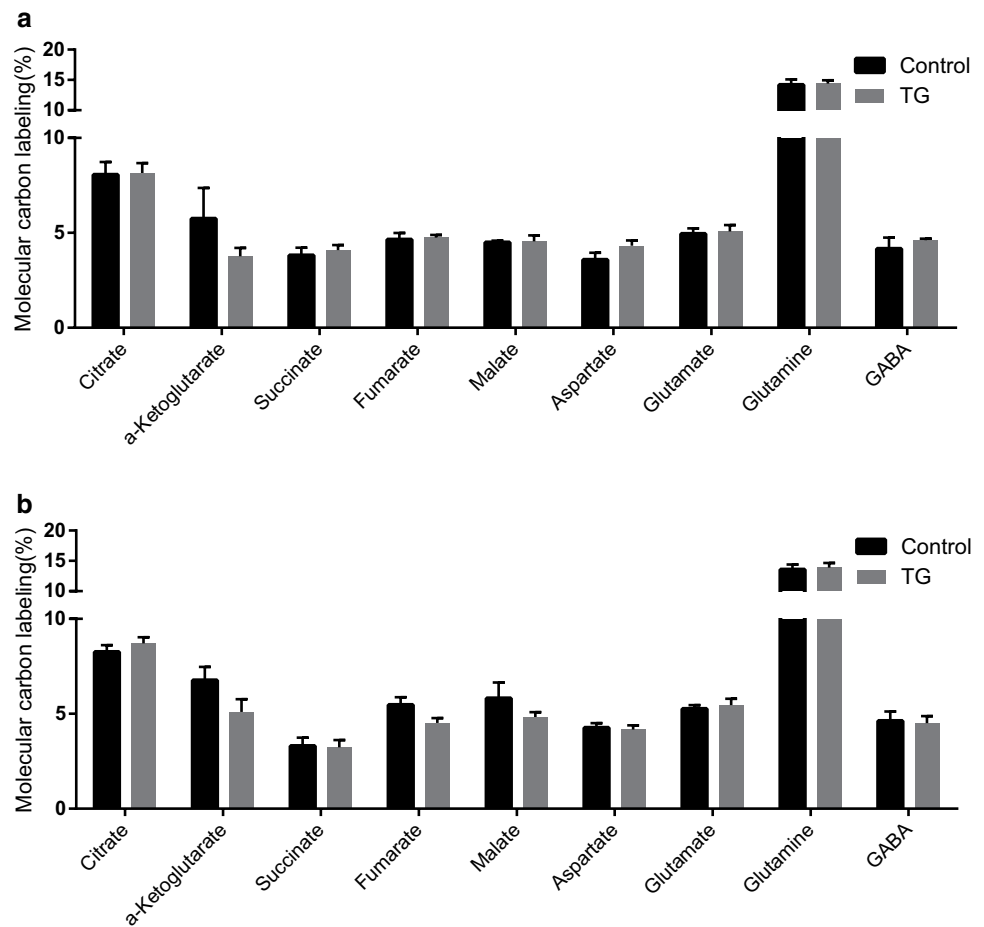
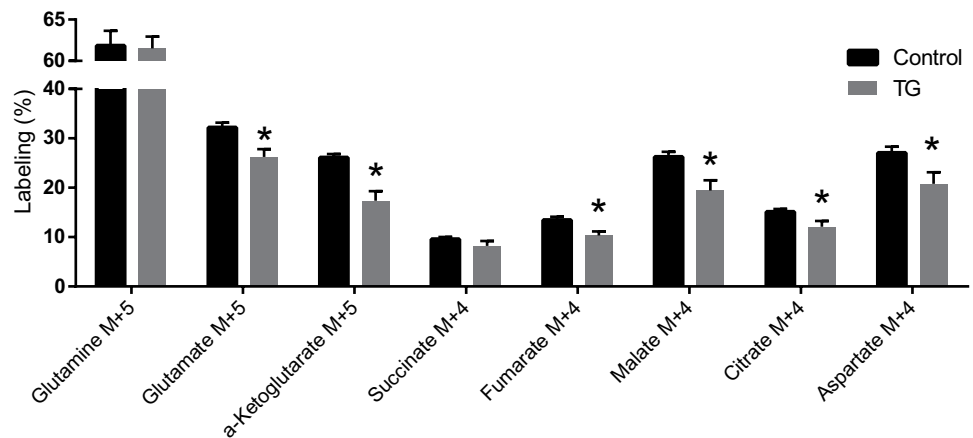


**Fig. 5**  $^{13}\text{C}$  Labeling from  $[U-^{13}\text{C}]$ glutamine metabolism. Labeling of TCA cycle intermediates and amino acids from incubations of cerebral cortical slices from wild-type control and APP<sup>sw</sup>/PSEN1<sup>dE9</sup> (TG) mice in media containing  $[U-^{13}\text{C}]$ glutamine. Results are presented as mean  $\pm$  SEM,  $n=4-5$ . Student's  $t$  test,  $p < 0.05$



### Hampered Oxidative Glutamine Metabolism in Cerebral Cortical Slices of APP<sup>sw</sup>/PSEN1<sup>dE9</sup> Mice

$^{13}\text{C}$  Labeling of amino acids and TCA cycle intermediates obtained from incubations of cerebral cortex slices from wild-type control and APP<sup>sw</sup>/PSEN1<sup>dE9</sup> mice in medium containing  $[U-^{13}\text{C}]$ glutamine are presented in Fig. 5.  $[U-^{13}\text{C}]$ Glutamine is mainly taken up by neurons, as

glutamine is released from astrocytes as part of the glutamate-glutamine cycle.

No significant difference was observed in glutamine M+5 enrichment between cerebral cortical slices from wild-type control and APP<sup>sw</sup>/PSEN1<sup>dE9</sup> mice. Glutamate M+5 enrichment, generated by deamidation of glutamine M+5, was in contrast significantly decreased in cerebral cortical slices of APP<sup>sw</sup>/PSEN1<sup>dE9</sup> mice

(18%). Glutamate M+5 is introduced into the TCA cycle as  $\alpha$ -ketoglutarate M+5. Significant decreases in labeling were observed for  $\alpha$ -ketoglutarate M+5 (33%), and several subsequent metabolites hereof, including: fumarate M+4 (23%), malate M+4 (26%), citrate M+4 (20%) and aspartate M+4 (23%). These results point towards a hampered oxidative metabolism of glutamine in cerebral cortical brain slices of APP<sup>sw</sup>/PSEN1<sup>de9</sup> mice.

### Decreased ATP Synthesis Rate of Cerebral Mitochondria from APP<sup>sw</sup>/PSEN1<sup>de9</sup> Mice

The changes in substrate utilization observed from incubations of brain slices could be a consequence of altered mitochondrial function. The ATP synthesis rate of isolated brain mitochondria from wild-type control and APP<sup>sw</sup>/PSEN1<sup>de9</sup> mice is presented in Fig. 6. A tendency towards significant lowering of the ATP synthesis rate is observed for brain mitochondria of APP<sup>sw</sup>/PSEN1<sup>de9</sup> mice when compared to wild-type controls, in the presence of malate and pyruvate ( $p=0.053$ ). This indicates a reduced cerebral mitochondrial ATP synthesis in APP<sup>sw</sup>/PSEN1<sup>de9</sup> mice prior to amyloid plaque deposition.

## Discussion

We present evidence of impaired cerebral cortical glucose metabolism and hampered TCA cycle metabolism in APP<sup>sw</sup>/PSEN1<sup>de9</sup> mice prior to significant amyloid plaque deposition. Additionally, reduced uptake and oxidative metabolism of glutamine was observed and whole-brain mitochondria of APP<sup>sw</sup>/PSEN1<sup>de9</sup> mice exhibit an impaired ATP synthesis rate.

### Altered Glycolytic Metabolism Precedes Amyloid Plaque Formation

In this study, we found increased labeling of intracellular lactate, alanine and first turn metabolites of the TCA

cycle, when incubating cerebral cortical slices of 3-month-old APP<sup>sw</sup>/PSEN1<sup>de9</sup> mice in a medium containing [U-<sup>13</sup>C]glucose. Since no significant changes in glial acetate metabolism were observed, this could indicate that the changes in [U-<sup>13</sup>C]glucose metabolism might primarily arise from alterations in neuronal energy metabolism. The augmented labeling was not matched by increased TCA cycle metabolism and oxidative phosphorylation. The increased labeling is likely explained by an elevated metabolism of [U-<sup>13</sup>C]glucose through glycolysis. Augmented glycolytic activity, which is not matched by oxidative phosphorylation, is known as aerobic glycolysis [17]. Interestingly, PET studies in AD patients have revealed enhanced aerobic glycolysis, which shows a regional correlation with amyloid deposits in the brain [18]. Elevated cerebral cortical levels of lactate have also been reported in APP transgenic mice when compared to wild-type controls, becoming significant with age [19]. These observations suggest that increased aerobic glycolysis in AD develops along with amyloid plaque formation. Furthermore, elevated amounts and labeling of lactate were reported in a transgenic rat model of AD upon injection of [1-<sup>13</sup>C]glucose [20], consistent with observations in AD patients [21]. Our findings are in line with these previous studies but suggest that the augmentation of aerobic glycolysis occurs prior to plaque deposition. Interestingly, it has been shown that enhanced glycolytic activity in neurons may lead to increased neuronal oxidative stress and death [22]. It can be speculated that the increased aerobic glycolysis might be a founding mechanism of neurodegeneration in AD. A significant enhancement of aerobic glycolysis would lead to increased lactate production. In this study, we only observed a tendency towards elevated amounts of lactate released to the media during incubation of cerebral cortical slices from APP<sup>sw</sup>/PSEN1<sup>de9</sup> mice. The elevated labeling of intracellular lactate and alanine could also arise from reduced conversion of [U-<sup>13</sup>C]pyruvate into [1,2-<sup>13</sup>C]acetylCoA catalyzed by PDH. Reduced PDH activity would lead to a buildup of [U-<sup>13</sup>C]pyruvate and hence increase the labeling of intracellular lactate and alanine, but have less effect on total lactate amounts compared to an elevated glycolytic flux. Hampered PDH activity is a recurrent observation in both AD patients and transgenic mouse models of AD [2, 4, 20, 23]. Since we only observed a tendency towards increased lactate release, our observations, may be explained by reduced PDH activity.

### Neuronal and Glial Implications in Early AD

AD is characterized by loss of neurons, but it is becoming evident that glial cells are highly affected in the AD brain as well [1, 24, 25]. From incubations with the glial substrate [1,2-<sup>13</sup>C]acetate, we found no changes in total glial acetate metabolism in the cerebral cortex and hippocampus

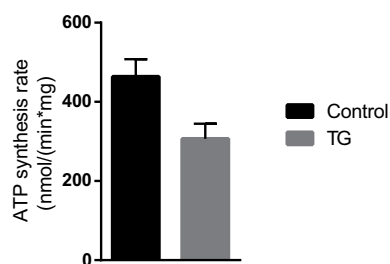


**Fig. 6** ATP synthesis rate of isolated brain mitochondria of wild-type control and APP<sup>sw</sup>/PSEN1<sup>de9</sup> (TG) mice. Results are presented as mean  $\pm$  SEM,  $n=3$ . Student's  $t$  test,  $p<0.05$

of APP<sup>swe</sup>/PSEN1<sup>dE9</sup> mice at 3 months of age. Several studies have shown that amyloid plaques lead to activation of astrocytes and microglia [24–26]. An elevated glial acetate metabolic rate has been reported in AD patients, which was attributed to increased neuroinflammation [27]. The unaltered glial acetate metabolism found in pre-plaque stage of APP<sup>swe</sup>/PSEN1<sup>dE9</sup> mice in this study is consistent with the key role of plaque-associated inflammation in glial metabolic changes.

Two major enzymes involved in the glutamate–glutamine cycle, the glutamine synthetase (GS) and phosphate-activated glutaminase (PAG), have been found to be altered in the brain of AD patients [28–30]. GS is located in astrocytes synthesizing glutamine from glutamate, while PAG is mainly located in neurons catalyzing the opposite reaction [11]. Concurrent with the loss of neurons observed in AD, an increased loss of PAG positive neurons have been found in postmortem human AD samples [31–33]. This could serve as an explanation for the decreased conversion of glutamine to glutamate observed in <sup>13</sup>C labeling from the incubations with [U-<sup>13</sup>C]glutamine. However, it should be kept in mind that the present study is conducted using an AD model at an early pathological stage. An alternative explanation of the reduced glutamine conversion could be linked to deficient TCA cycle metabolism. As shown from the incubations with [U-<sup>13</sup>C]glucose, cerebral cortical slices of APP<sup>swe</sup>/PSEN1<sup>dE9</sup> mice exhibit reduced TCA cycle activity. Glutamate can be converted into  $\alpha$ -ketoglutarate and thereby act as substrate for the TCA cycle. Decreased TCA cycle activity might reduce the need of introduction of  $\alpha$ -ketoglutarate into the cycle. This would lower the need for deamidation of glutamine into glutamate and lower the <sup>13</sup>C labeling of glutamate M + 5. The alterations in labeling observed from metabolism of [U-<sup>13</sup>C]glutamine could therefore be reflections of hampered neuronal TCA cycle activity. The reduced glutamine uptake and potential alterations in PAG activity could impair homeostasis of the glutamate–glutamine cycle and directly affect neurotransmission. Our results suggest that reduced glutamine uptake and hampered oxidative glutamine metabolism could be very early markers of AD pathogenesis as they precede amyloid plaque formation in APP<sup>swe</sup>/PSEN1<sup>dE9</sup> mice.

### Mitochondrial Dysfunction in Early AD

Here we present results, indicating decreased ATP synthesis rate in isolated cerebral mitochondria from APP<sup>swe</sup>/PSEN1<sup>dE9</sup> mice at 3 months of age. Changes in mitochondrial function are considered to play a crucial role for the development of AD [2, 12, 13]. Reductions in activity or expression of cytochrome c oxidase (Complex IV of the electron transport chain) and PDH are recurrent observations in the AD brain [2, 4]. Furthermore, decreased activity

of key TCA cycle enzymes have been reported from human AD patients [34]. Such mitochondrial alternations lead to decreased oxidative phosphorylation and compromise cellular energy homeostasis.

Several studies have reported mitochondrial changes in early stages of AD pathogenesis [23, 35, 36]. Our observations of decreased ATP synthesis may be explained by hampered PDH activity as described above, as this additionally would dampen oxidative metabolism and hence decrease mitochondrial ATP synthesis. Significant reductions in both ATP levels and expression of cytochrome c oxidase and PDH before amyloid plaque formation have been shown in several transgene animal models of AD [23, 35–38]. These observations are in line with our results, as we observe that the mitochondrial ATP synthesis rate in the brain of APP<sup>swe</sup>/PSEN1<sup>dE9</sup> mice show a tendency towards being compromised prior to amyloid plaque deposition.

### Conclusions

We show that brain energy metabolism is affected in APP<sup>swe</sup>/PSEN1<sup>dE9</sup> mice prior to amyloid plaque deposition. Cerebral cortical slices exhibits changes in glucose metabolism, reduced TCA cycle activity and impaired uptake and oxidative metabolism of glutamine. Furthermore, a tendency towards decreased ATP synthesis rate was observed in isolated brain mitochondria. These results demonstrate that several specific alterations in cerebral energy metabolism precede the key pathological hallmark of amyloid plaques in APP<sup>swe</sup>/PSEN1<sup>dE9</sup> mice.

**Acknowledgments** The competent laboratory assistance of Catia Andersen is cordially acknowledged. The Lundbeck Foundation and the Scholarship of Peter & Emma Thomsen are acknowledged for their financial support to JVA.

**Author contributions** All authors designed the experiments. JVA, SKC, BIA, and JDN performed the experiments and analyzed the data. JVA and HSW wrote the article. All authors have provided constructive input and have approved the final manuscript.

### Compliance with Ethical Standards

**Conflict of Interest** The authors have nothing to declare.

### References

1. De Strooper B, Karran E (2016) The Cellular Phase of Alzheimer's Disease. *Cell* 164(4):603–615. doi:10.1016/j.cell.2015.12.056
2. Gibson GE, Shi Q (2010) A mitocentric view of Alzheimer's disease suggests multi-faceted treatments. *J Alzheimers Dis* 20(Suppl 2):S591–S607. doi:10.3233/jad-2010-100336
3. Mosconi L, Pupi A, De Leon MJ (2008) Brain glucose hypometabolism and oxidative stress in preclinical Alzheimer's disease. *Ann N Y Acad Sci* 1147:180–195. doi:10.1196/annals.1427.007



4. Blass JP, Sheu RK, Gibson GE (2000) Inherent abnormalities in energy metabolism in Alzheimer disease. Interaction with cerebrovascular compromise. *Ann N Y Acad Sci* 903:204–221
5. Jankowsky JL, Fadale DJ, Anderson J, Xu GM, Gonzales V, Jenkins NA, Copeland NG, Lee MK, Younkin LH, Wagner SL, Younkin SG, Borchelt DR (2004) Mutant presenilins specifically elevate the levels of the 42 residue beta-amyloid peptide in vivo: evidence for augmentation of a 42-specific gamma secretase. *Hum Mol Genet* 13(2):159–170. doi:[10.1093/hmg/ddh019](https://doi.org/10.1093/hmg/ddh019)
6. Garcia-Alloza M, Robbins EM, Zhang-Nunes SX, Purcell SM, Betensky RA, Raju S, Prada C, Greenberg SM, Bacskai BJ, Frosch MP (2006) Characterization of amyloid deposition in the APPsw/PS1dE9 mouse model of Alzheimer disease. *Neurobiol Dis* 24(3):516–524. doi:[10.1016/j.nbd.2006.08.017](https://doi.org/10.1016/j.nbd.2006.08.017)
7. Lalonde R, Kim HD, Maxwell JA, Fukuchi K (2005) Exploratory activity and spatial learning in 12-month-old APP(695)SWE/co + PS1/DeltaE9 mice with amyloid plaques. *Neurosci Lett* 390(2):87–92. doi:[10.1016/j.neulet.2005.08.028](https://doi.org/10.1016/j.neulet.2005.08.028)
8. Savonenko A, Xu GM, Melnikova T, Morton JL, Gonzales V, Wong MP, Price DL, Tang F, Markowska AL, Borchelt DR (2005) Episodic-like memory deficits in the APPsw/PS1dE9 mouse model of Alzheimer's disease: relationships to beta-amyloid deposition and neurotransmitter abnormalities. *Neurobiol Dis* 18(3):602–617. doi:[10.1016/j.nbd.2004.10.022](https://doi.org/10.1016/j.nbd.2004.10.022)
9. Minkeviciene R, Ihalainen J, Malm T, Matilainen O, Keksa-Goldsteine V, Goldsteins G, Iivonen H, Leguit N, Glennon J, Koistinaho J, Banerjee P, Tanila H (2008) Age-related decrease in stimulated glutamate release and vesicular glutamate transporters in APP/PS1 transgenic and wild-type mice. *J Neurochem* 105(3):584–594. doi:[10.1111/j.1471-4159.2007.05147.x](https://doi.org/10.1111/j.1471-4159.2007.05147.x)
10. Minkeviciene R, Rheims S, Dobszay MB, Zilberter M, Hartikainen J, Fulop L, Penke B, Zilberter Y, Harkany T, Pitkanen A, Tanila H (2009) Amyloid beta-induced neuronal hyperexcitability triggers progressive epilepsy. *J Neurosci* 29(11):3453–3462. doi:[10.1523/jneurosci.5215-08.2009](https://doi.org/10.1523/jneurosci.5215-08.2009)
11. Bak LK, Schousboe A, Waagepetersen HS (2006) The glutamate/GABA-glutamine cycle: aspects of transport, neurotransmitter homeostasis and ammonia transfer. *J Neurochem* 98(3):641–653. doi:[10.1111/j.1471-4159.2006.03913.x](https://doi.org/10.1111/j.1471-4159.2006.03913.x)
12. Blass JP (2001) Brain metabolism and brain disease: is metabolic deficiency the proximate cause of Alzheimer dementia? *J Neurosci Res* 66(5):851–856
13. Moreira PI, Carvalho C, Zhu X, Smith MA, Perry G (2010) Mitochondrial dysfunction is a trigger of Alzheimer's disease pathophysiology. *Biochim Biophys Acta* 1802(1):2–10. doi:[10.1016/j.bbadis.2009.10.006](https://doi.org/10.1016/j.bbadis.2009.10.006)
14. Walls AB, Bak LK, Sonnewald U, Schousboe A, Waagepetersen HS (2014) Metabolic Mapping of Astrocytes and Neurons in Culture Using Stable Isotopes and Gas Chromatography-Mass Spectrometry (GC-MS). In: Hirrlinger J, Waagepetersen HS (eds) *Brain Energy Metabolism*, vol 90. Humana Press, New York
15. Sonnewald U, Westergaard N, Schousboe A, Svendsen JS, Unsgard G, Petersen SB (1993) Direct demonstration by [<sup>13</sup>C] NMR spectroscopy that glutamine from astrocytes is a precursor for GABA synthesis in neurons. *Neurochem Int* 22(1):19–29
16. Amaral AI, Hadera MG, Tavares JM, Kotter MR, Sonnewald U (2016) Characterization of glucose-related metabolic pathways in differentiated rat oligodendrocyte lineage cells. *Glia* 64(1):21–34. doi:[10.1002/glia.22900](https://doi.org/10.1002/glia.22900)
17. Vaishnavi SN, Vlassenko AG, Rundle MM, Snyder AZ, Mintun MA, Raichle ME (2010) Regional aerobic glycolysis in the human brain. *Proc Natl Acad Sci USA* 107(41):17757–17762. doi:[10.1073/pnas.1010459107](https://doi.org/10.1073/pnas.1010459107)
18. Vlassenko AG, Vaishnavi SN, Couture L, Sacco D, Shannon BJ, Mach RH, Morris JC, Raichle ME, Mintun MA (2010) Spatial correlation between brain aerobic glycolysis and amyloid-beta (Aβ) deposition. *Proc Natl Acad Sci USA* 107(41):17763–17767. doi:[10.1073/pnas.1010461107](https://doi.org/10.1073/pnas.1010461107)
19. Harris RA, Tindale L, Lone A, Singh O, Macauley SL, Stanley M, Holtzman DM, Bartha R, Cumming RC (2016) Aerobic Glycolysis in the Frontal Cortex Correlates with Memory Performance in Wild-Type Mice But Not the APP/PS1 Mouse Model of Cerebral Amyloidosis. *J Neurosci* 36(6):1871–1878. doi:[10.1523/jneurosci.3131-15.2016](https://doi.org/10.1523/jneurosci.3131-15.2016)
20. Nilsen LH, Witter MP, Sonnewald U (2014) Neuronal and astrocytic metabolism in a transgenic rat model of Alzheimer's disease. *J Cereb Blood Flow Metab* 34(5):906–914. doi:[10.1038/jcbfm.2014.37](https://doi.org/10.1038/jcbfm.2014.37)
21. Lin AP, Shic F, Enriquez C, Ross BD (2003) Reduced glutamate neurotransmission in patients with Alzheimer's disease—an in vivo (<sup>13</sup>C) magnetic resonance spectroscopy study. *MAGMA* 16(1):29–42. doi:[10.1007/s10334-003-0004-x](https://doi.org/10.1007/s10334-003-0004-x)
22. Herrero-Mendez A, Almeida A, Fernandez E, Maestre C, Moncada S, Bolanos JP (2009) The bioenergetic and antioxidant status of neurons is controlled by continuous degradation of a key glycolytic enzyme by APC/C-Cdh1. *Nat Cell Biol* 11(6):747–752. doi:[10.1038/ncb1881](https://doi.org/10.1038/ncb1881)
23. Yao J, Irwin RW, Zhao L, Nilsen J, Hamilton RT, Brinton RD (2009) Mitochondrial bioenergetic deficit precedes Alzheimer's pathology in female mouse model of Alzheimer's disease. *Proc Natl Acad Sci USA* 106(34):14670–14675. doi:[10.1073/pnas.0903563106](https://doi.org/10.1073/pnas.0903563106)
24. Kamphuis W, Orre M, Kooijman L, Dahmen M, Hol EM (2012) Differential cell proliferation in the cortex of the APPswPS1dE9 Alzheimer's disease mouse model. *Glia* 60(4):615–629. doi:[10.1002/glia.22295](https://doi.org/10.1002/glia.22295)
25. Steele ML, Robinson SR (2012) Reactive astrocytes give neurons less support: implications for Alzheimer's disease. *Neurobiol Aging* 33(2):423.e421–413. doi:[10.1016/j.neurobiolaging.2010.09.018](https://doi.org/10.1016/j.neurobiolaging.2010.09.018)
26. Ordonez-Gutierrez L, Anton M, Wandosell F (2015) Peripheral amyloid levels present gender differences associated with aging in AbetaPP/PS1 mice. *J Alzheimers Dis* 44(4):1063–1068. doi:[10.3233/jad-141158](https://doi.org/10.3233/jad-141158)
27. Sailasuta N, Harris K, Tran T, Ross B (2011) Minimally invasive biomarker confirms glial activation present in Alzheimer's disease: a preliminary study. *Neuropsychiatr Dis Treat* 7:495–499. doi:[10.2147/ndt.s23721](https://doi.org/10.2147/ndt.s23721)
28. Walton HS, Dodd PR (2007) Glutamate-glutamine cycling in Alzheimer's disease. *Neurochem Int* 50(7–8):1052–1066. doi:[10.1016/j.neuint.2006.10.007](https://doi.org/10.1016/j.neuint.2006.10.007)
29. Robinson SR (2000) Neuronal expression of glutamine synthetase in Alzheimer's disease indicates a profound impairment of metabolic interactions with astrocytes. *Neurochem Int* 36(4–5):471–482
30. Kulijewicz-Nawrot M, Sykova E, Chvatal A, Verkhatsky A, Rodriguez JJ (2013) Astrocytes and glutamate homeostasis in Alzheimer's disease: a decrease in glutamine synthetase, but not in glutamate transporter-1, in the prefrontal cortex. *ASN Neuro* 5(4):273–282. doi:[10.1042/an20130017](https://doi.org/10.1042/an20130017)
31. McGeer EG, McGeer PL, Akiyama H, Harrop R (1989) Cortical glutaminase, beta-glucuronidase and glucose utilization in Alzheimer's disease. *Can J Neurol Sci* 16(4 Suppl):511–515
32. Burbueva G, Boksha IS, Tereshkina EB, Savushkina OK, Prokhorova TA, Vorobyeva EA (2014) Glutamate and GABA-metabolizing enzymes in post-mortem cerebellum in Alzheimer's disease: phosphate-activated glutaminase and glutamic acid decarboxylase. *Cerebellum* 13(5):607–615. doi:[10.1007/s12311-014-0573-4](https://doi.org/10.1007/s12311-014-0573-4)
33. Akiyama H, McGeer PL, Itagaki S, McGeer EG, Kaneko T (1989) Loss of glutaminase-positive cortical neurons in Alzheimer's disease. *Neurochem Res* 14(4):353–358

34. Bubber P, Haroutunian V, Fisch G, Blass JP, Gibson GE (2005) Mitochondrial abnormalities in Alzheimer brain: mechanistic implications. *Ann Neurol* 57(5):695–703. doi:[10.1002/ana.20474](https://doi.org/10.1002/ana.20474)
35. Hauptmann S, Scherping I, Droese S, Brandt U, Schulz KL, Jendrach M, Leuner K, Eckert A, Muller WE (2009) Mitochondrial dysfunction: an early event in Alzheimer pathology accumulates with age in AD transgenic mice. *Neurobiol Aging* 30(10):1574–1586. doi:[10.1016/j.neurobiolaging.2007.12.005](https://doi.org/10.1016/j.neurobiolaging.2007.12.005)
36. Du H, Guo L, Yan S, Sosunov AA, McKhann GM, Yan SS (2010) Early deficits in synaptic mitochondria in an Alzheimer's disease mouse model. *Proc Natl Acad Sci USA* 107(43):18670–18675. doi:[10.1073/pnas.1006586107](https://doi.org/10.1073/pnas.1006586107)
37. Zhang C, Rissman RA, Feng J (2015) Characterization of ATP alternations in an Alzheimer's disease transgenic mouse model. *J Alzheimers Dis* 44(2):375–378. doi:[10.3233/jad-141890](https://doi.org/10.3233/jad-141890)
38. Pedros I, Petrov D, Allgaier M, Sureda F, Barroso E, Beas-Zarate C, Auladell C, Pallas M, Vazquez-Carrera M, Casadesus G, Folch J, Camins A (2014) Early alterations in energy metabolism in the hippocampus of APP<sup>swe</sup>/PS1<sup>dE9</sup> mouse model of Alzheimer's disease. *Biochim Biophys Acta* 1842(9):1556–1566. doi:[10.1016/j.bbadis.2014.05.025](https://doi.org/10.1016/j.bbadis.2014.05.025)